

Capturing the 3D secrets of a flickering candle based on digital holographic microscopy

Shaohan Qin

The Experimental High School Attached to Beijing Normal University, Beijing, China

austinqy2007@163.com

Abstract. The temperature distribution of flames has long been a fascinating topic of study. To quantitatively analyze the temperature field of flames, traditional methods include infrared devices, thermocouples and thermometer. However, these conventional techniques provide only cross-sectional snapshots while lacking the capability to offer real-time 3D temperature field visualization. This paper proposed a different approach to measure the 3D temperature field with accurate data and details by applying the digital holography. First, based on digital holography and the equations of thermodynamics, we derived the equation between the phase difference and temperature. Then we built a transmission off-axis digital holographic microscopy in the experimental section to perform static and dynamic flame measurements. To calibrate the actual temperatures and test our theory's accuracy, we also took photographs of the flames as a standard reference using an infrared thermal imager. Finally, we obtained a quantitative 3D distribution of the temperature field and a qualitative dynamic process of 3D temperature field. Our results show that the temperature decreases from the center of the flame and follows a general pattern. The comparison with infrared imaging shows that digital holography offers an accurate measurement of the temperature.

Keywords: Computational Imaging, Digital Holographic Microscopy, Temperature Field, 3D Measurement

1. Introduction

Digital holography is an imaging technique that allows us to capture and reconstruct the three-dimensional information of an object using digital sensors and computational algorithms. The process involves several steps, including capturing the hologram, performing numerical reconstruction, and visualizing the reconstructed object. The concept of holography was introduced by Dennis Gabor in 1947, but it was not until 1962 that the first laser holograms were created by Emmett Leith and Juris Upatnieks [1,2]. In the 1990s, advancements in computing power and digital imaging technologies enabled the development of digital holography. With the use of Charged-coupled Device (CCD) and Complementary Metal Oxide Semiconductor (CMOS), holograms could be digitally recorded and reconstructed using numerical algorithms [3]. In the early 2000s, digital Fourier holography emerged as a prominent technique in digital holography. Another important development in digital holography was phase-shifting digital holography [4,5]. Over the years, researchers have further refined the mathematical and computational methods used in digital holography [6,7]. This has led to improvements in image quality, reduction of artifacts, and the ability to handle complex samples.

Inspired by these researches, this paper will focus on how to measure the temperature field of static and growing flames using digital holography. We will first introduce the theory of digital holography measurement [8,9]. Then we will discuss the relationship between the temperature and the index of refraction, which is crucial to the measurement of temperature. Next, we will go into the algorithm associated with digital holography. After the theoretical discussion, we will introduce our experimental setup and data analysis. To verify the accuracy of the results obtained using DHM, we propose comparing our findings with infrared images of the flames. Such a comparison would directly prove the validity or shortcomings of the paper's results, providing evidence for the reliability of DHM as a method for measuring the temperature field of flames.

To theoretically derive the algorithm for digital holography, we first need to analyze the interference recording process. Writing out the wave equation for the two beams of light, the object wave can be expressed as

$$O(x, y) = o(x, y) \exp[-j\phi(x, y)] \quad (1)$$

Where j is the imaginary unit. Similarly, the reference wave can be expressed as

$$R(x, y) = r(x, y) \exp[-j\phi(x, y)] \quad (2)$$

When the two waves meet and interfere at the front of the receiving CCD, we can mathematically write down the intensity of the interference pattern as the combination of the two waves

$$I(x, y) = |O(x, y) + R(x, y)|^2 = |O(x, y)|^2 + |R(x, y)|^2 + R^*(x, y)O(x, y) + R(x, y)O^*(x, y) \quad (3)$$

The first two terms in the equation above are the intensity of the object and reference light wave, independent of the phase, so it represents the 0th order image, and thus is the 0th order spectrum in the spectrogram. The third term is the product of the complex conjugate of the object wave and the reference wave, representing object wave traveling in the direction of the reference wave, so it is the -1 order spectrum in the spectrogram. Similarly, the last term is the product of the object wave and the complex conjugate of the reference wave, representing the object wave traveling in the opposite direction as the reference wave, so it is the +1 order spectrum in the spectrogram.

When the interference pattern gets recorded by the CCD or CMOS, the data gets processed using the *rect* and *comb* function.

$$I(m, n) = I(x, y) \text{comb}\left(\frac{x}{\Delta x}, \frac{y}{\Delta y}\right) \text{rect}\left(\frac{x}{M \times \Delta x}, \frac{y}{N \times \Delta y}\right) \quad (4)$$

For our purpose of reconstructing a hologram over a relatively small distance, we will adopt the angular spectrum algorithm, which is the most efficient way that suits our purpose.

$$U(f_x, f_y) = C(f_x, f_y) I(f_x, f_y) H(f_x, f_y) \quad (5)$$

Where f represents the spatial frequency, C is the reproduced light wave, I is the hologram, H is the spatial propagation equation which can be expressed as

$$H(f_x, f_y) = e^{j\frac{2\pi}{\lambda}z} \sqrt{1 - (\lambda f_x)^2 - (\lambda f_y)^2} \quad (6)$$

Next, we will derive the relationship between temperature and index of refraction. By using the Lorentz-Lorenz formula and the Gladstone-Dale equation, we can find that

$$\frac{n - 1}{\rho} = K \quad (7)$$

Where K is the Gladstone-Dale constant, which changes according to the specific kind of air and the wavelength of the light. Combining this with the ideal gas law, we have

$$\frac{1}{T} - \frac{1}{T_0} = \frac{R}{PKM} (n_T - n_{\text{air}})$$

$$n_T = 1 + \frac{0.78729}{T} \quad (8)$$

Where T_0 is the surrounding temperature, T is the temperature of the medium of refraction, and n_T is the index of refraction.

To find out the effect of the index of refraction on the phase difference, we'll use a simple diagram (Figure 1).

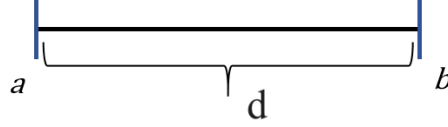


Figure 1. Schematic diagram of the phase difference

Consider a very small distance ab . When there's nothing between a and b , the optical path is $n_{air}d$. Where d is the geometric difference between ab .

When a flame is put between a and b , the optical path changes to n_Td . So the difference in optical path is

$$\Delta\varphi = kd(n_T - n_{air}) \quad (9)$$

Where n_T can be derived from the previous discussion. This shows the phase difference and the difference between index of refraction follow a linear relationship, which in turn allows us to find out the relationship between phase difference and temperature. Using equation (8), we can get

$$\Delta\varphi = kd \left(1 + \frac{0.78729}{T} - n_{air} \right) \quad (10)$$

This is thus the relationship between phase difference and temperature. With this relationship, we will be able to measure the temperature distribution of candle flames, since difference in temperature leads to a phase difference, which can then be measured in the interference patterns in the holograms.

2. Methods

In the classic optical paths like the Michelson light path and the Mach-Zehnder path way, equipment include a laser to produce the light that captures the object's information and forms the interference pattern, reflective lens to reflect the light, beam-splitting prisms (BS) to separate light, convex lens for beam expansion and focusing, and finally the CCD, or CMOS, at the back of the light path to record the information. For this particular experiment, we chose the Mach-Zehnder light path because of its simplicity and convenience. All the hardware and equipment were provided by Tsinghua University except for the candles, the adjustable platform and other minor gadgets. For the laser, we had a green laser device with a wavelength of 532 nm and maximum power output of 0.5~1mW. Two reflective lenses and two BS were adopted for the experiment. Two convex lenses with focal length of 10cm, a pinhole filter with the diameter of 50 μ m, and a CCD with pixel size of 5.4 μ m were also used.

The schematic and actual picture of our optical system is separately shown in Figure 2 and Figure3. The laser emits a beam of light that goes through the small pinhole in front of it. There, it gets narrowed into a single point, and as a point source, it then goes on to expand as a spherical wave through the effect of the convex lens. As the light beam gets expanded, it passes through a beam-splitting prism, sending one beam of light through, while reflecting the rest of the light. The light that passes through this BS is called the object light wave because it then passes the object, the flame. After this, the object's light wave meets a reflective lens, where it gets deflected downwards. As for the light wave that gets reflected at the first BS, it meets a reflective lens and is reflected. It then meets with the reflected object light, and the combined light travels to the CCD, where it is recorded.

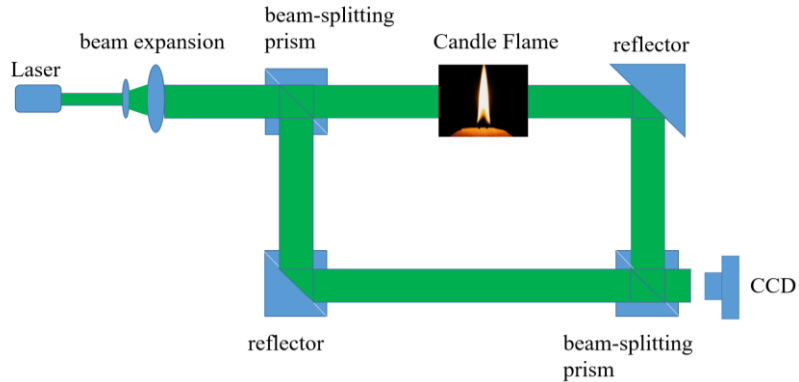


Figure 2. Schematic diagram of optical path structure



Figure 3. Mach-Zehnder optical path

Here is the detailed experimental procedure.

Gather all the needed experimental equipment on the table, and connect the CCD to the computer.

Arrange everything to create the general light path and adjust all equipment so that they have the same height.

Adjust the pinhole so that the laser can precisely pass through it, which turns the light into a spherical light wave.

(4) Construct the Mach-Zehnder interferometric light path.

(5) Adjust the distance between all equipment to have a full image on the CCD.

(6) Put in the candle, so that the light source is aligned with the candle wick; connect the CCD, and open the software. Light the candle and start recording, setting the time interval of the snapshot to be sufficiently small. Data collected right after the lighting of the candle are categorized as the dynamic experiment, whereas data collected after the candle flame has become steady are put in the static experiment.

(7) Open the MindVision software and observe whether there is an interference fringe hologram. Observe the spectrogram and adjust the angle of the reflector and beam-splitting prisms, so that the ± 1 order image and the zero-order image can be differentiated.

(8) Process the data collected on the computer via software provided by Tsinghua physics department. Use the 3D picture of the light field, and use the relationship between phase difference and temperature to transform the light field into the temperature field.

3. Results

For our experiment, we set up the needed equipment and arranged them into the desired optical path. Then we took the hologram of the candle flame. After data processing, we can get the needed results.

Static experiment: For the first experiment, we will measure the temperature field of a steadily burning flame on a candle. First, we capture the hologram. Then we use the photo processing software and the MATLAB code, combining which, we get pictures of the entire process of digital holography. The Fourier transform is applied to the hologram and the +1 order image is truncated as shown in Figure 4.

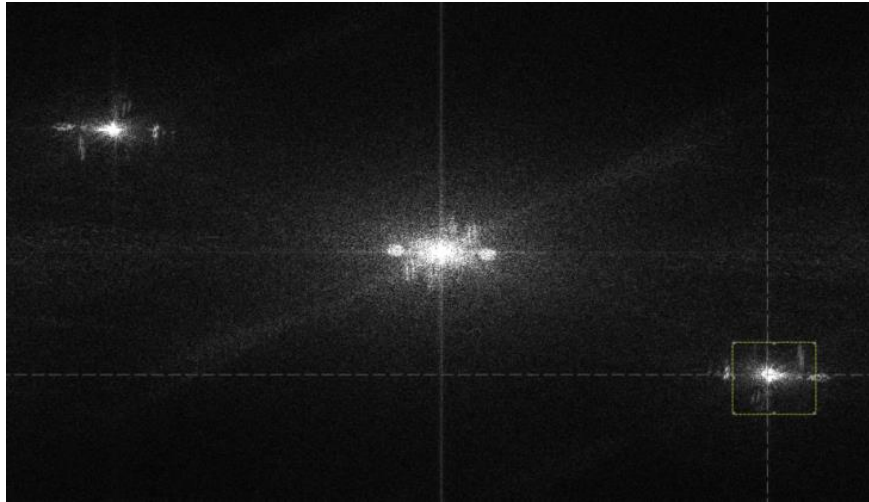


Figure 4. Spectrogram of a static candle flame

After the phase unwrapping process, the resulting phase diagram is shown in Figure 5. It shows the two dimensional cross-sectional view and the three dimensional view of the phase diagram. The figure is unwrapped, which means it shows the original phase difference. But without calibrating, it doesn't exactly reflect temperature. To have the temperature, we need to calibrate figure 5 and transform it to the real temperature data. We can thus have the experimental results for a steadily burning fire. The 3D temperature field can be appreciated directly without any delay.

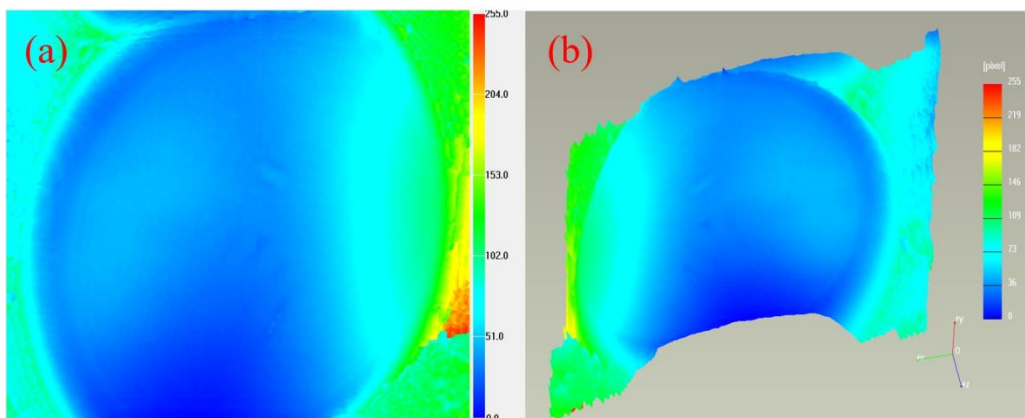


Figure 5. Unwrapped phase image of the candle flame: (a) 2D view, (b) 3D view

From figure 5 , we can find the qualitative shape of the candle temperature field. To validate its accuracy, we will compare the measurement of the shaped candle temperature field with the results from an infrared thermal imager. The infrared measurement of temperature is shown in Figure 6. It

shows the cross-sectional view of the temperature distribution of the flame with the temperature scale on the right.

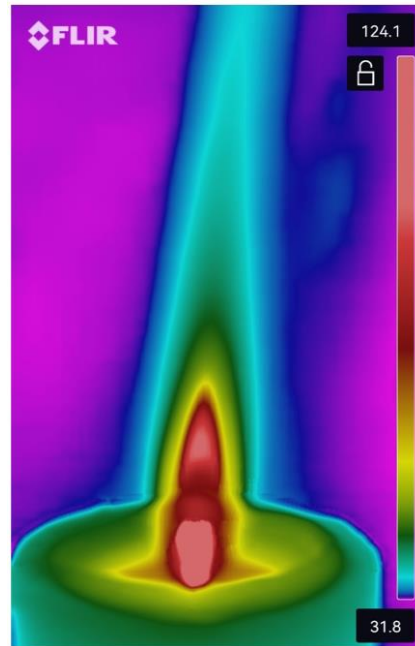


Figure 6. Infrared measurement of the candle temperature

Here taking the highest temperature of the infrared measurement of the candle temperature as the reference equivalent to the highest value of the phase diagram, the approximate 3D temperature field based on digital holographic microscopy measurement can be obtained as below (Figure 7). Through Figure 7, we can quantitatively see the three-dimensional shape of the candle flame temperature field, and more intuitively see the internal distribution law of the temperature field. The central core of the flame has a relatively lower temperature than the outer part, but the temperature decreases as we get further away from the centre of the flame. So generally the temperature decreases from inside to outside, and the area of relatively low temperature is probably because it is actually the string of the candle and not the fire.

Subject to the limitations of this paper, we can only show the cross-sectional view of the temperature field. In actual MATLAB and software processing, we can rotate the 3D field to get the full 3D shape.

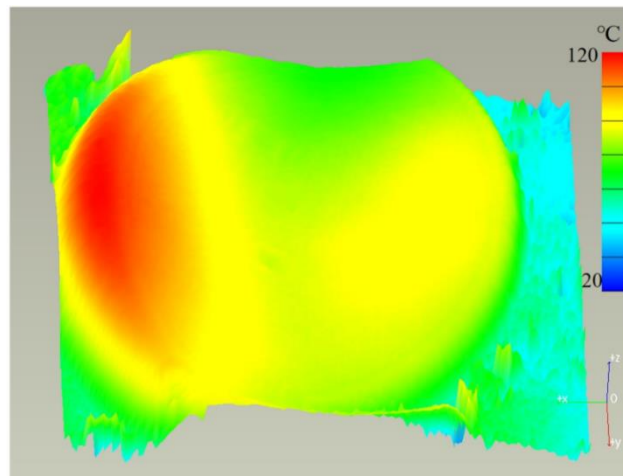


Figure 7. The finalized three-dimensional temperature field of the candle flame

Dynamic experiments: Through static experiments we can get the instantaneous three-dimensional distribution of the candle temperature field. In the dynamic experiment, we will explore how fires grow after being lit. We will set the camera to take pictures every 0.2-second interval to record in real time the process of the candle from the unlit state to the flame getting bigger gradually. It is equivalent to repeating the process of previous experiment several times, recording the complete dynamic process.

For this part, we were able to get a wrapped image of the growing flame. But when trying to unwrap the image, we encountered some difficulties. The results from using the discrete cosine transform (DCT) method proved unsuccessful due to the rapidly changing shape of the fire. Therefore, we didn't do the phase unwrapping process in this part of the experiment, though it does not prevent us from getting a quantitative image of the flame's shape. The wrapped images are shown below.

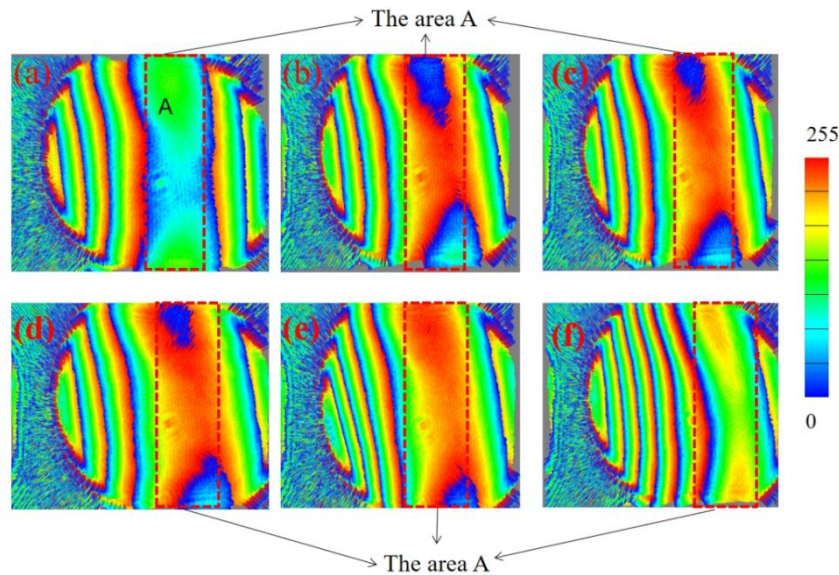


Figure 8. Wrapped phase image of the candle flame. (a)-(f): Time progress by 0.2 seconds in sequence

In the static experiment, by looking at the unwrapped image of the flame, we can see that its temperature is divided into different layers, with the heart of the flame being the highest in temperature, which corresponds to the result from the infrared thermal imager. The temperature actually decreases as we move farther away from the centre of the flame. The layers all have a similar geometric pattern, taking on the form of sharp oval-like shape of the actual visible flame. For the dynamic experiment, by studying the area A, we can see qualitatively how the flame expands. It can be observed that the temperature field is generally the same as the static experiment. From the wrapped image of the flame, we can see that as time goes on, the various layers become thinner, and the specific temperature of the middle of the flame, which is in the area A, also changes with time. The flame grows larger, the gradient of the temperature field becomes larger too.

4. Discussion

In our daily life, we used to consider the temperature of a candle flame as increasing from center to the outmost layer. However, with the specific candle and the measurement method in this experiment, we found that the temperature of the inner layer of the flame is actually highest. But this result needs to be tested again in a more generalized situation.

For future studies, we would like to see how to more accurately calculate the temperature field using better algorithms and fewer approximations. Also, we want to adjust our experimental setup so that we can capture a more complete image of the flame. Specific effects of noise and other factors which may cause inaccuracy should be taken into consideration. To make the data processing period

shorter so that the results of the temperature field can be obtained instantaneously, we can look to building a more convenient device that can process the data itself using the algorithms.

5. Conclusion

To measure the 3D temperature field of a burning candle flame, this paper discussed the theory of digital holography, including the interference, diffraction and transmission of light, introducing the object, recording, and reconstruction planes. Then, we used thermal physics to derive the relationship between temperature and the index of refraction. Thus, by using the angular spectrum algorithm, we were able to reconstruct the information recorded by the light wave into the 3D temperature field. This approach possessed advantages in offering three-dimensional view of the flame and real-time measurements compared to infrared and other interference methods. In our experiment, we evaluated our theory and measured the temperature field of both steadily burning flame and growing flame. As a complementary experiment, we took the temperature image of the candle flame using an infrared thermal imager. This not only acts as a calibration but also provides validation for our DHM theory. We were able to get the temperature field of a burning candle both experimentally and theoretically, helping us better understand how exactly a flame is layered, and how fire expands after being lit. This paper also aimed to simplify the otherwise complex and expensive optical path without affecting its accuracy. The relatively simple optical path we built met this goal.

Apart from this study, digital holography can have many other far-reaching applications. It can measure not only temperature field, but also other fields in three dimensions. For example, using the same theory discussed in this paper, we can measure the leak of coal mine gas, using the phase difference to calculate the concentration of the coal mine gas.

References

- [1] Goodman D. S., 1984. Illuminator for Dark Field Microscopy. *Applied Optics*, 23(16).
- [2] D. Gabor, 1948. A New Microscopic Principle. *Nature*, 161(4098), 777-778.
- [3] D. Gabor, 1949. Microscopy by Reconstructed Wave-Fronts. *Proceedings of the Royal Society A Mathematical Physical & Engineering Sciences*, 197(1051):454-487.
- [4] L. Onural, P.D. Scott, 1986. Digital Decoding of In-line Holograms for Imaging Fractal Aggregates. *Electronics Letters*, 22(21):1118-1119.
- [5] G. Liu, P. D. Scott, 1987. Phase Retrieval and Two-image Elimination for In-line Fresnel Holograms. *Journal of the Optical Society of America A*, 4(1):159-165.
- [6] Waleed S. Haddad, David Cullen, Johndale C. Solem, 1991. Fourier-transform Holographic Microscope. *International Society for Optics and Photonics*.
- [7] U. Schnars and W. Juptner, 1993. Principles of Direct Holography for Interferometry. Presented at the Proc. 2nd Int. Workshop on Automatic Processing of Fringe Patterns Bremen.
- [8] Roman Doleček, Pavel Psota, Vít Lédl, Tomáš Vít, Jan Václavík, and Václav Kopecký. 2013. General temperature field measurement by digital holography. *Applied Optics*, 52(1), A319-A325.
- [9] P. Marquet, B. Rappaz, P. Magistretti, E. Cuche, Y. Emery, T. Colomb, and C. Depeursinge, 2005. Digital holographic microscopy: a noninvasive contrast imaging technique allowing quantitative visualization of living cells with subwavelength axial accuracy. *Optics Letters*, 30(5), 468-470.